Case Studies in Thermal Engineering 64 (2024) 105562

Contents lists available at ScienceDirect

Case Studies in Thermal Engineering

journal homepage: www.elsevier.com/locate/csite

Artificial intelligence based emission and performance prediction, and optimization of HHO-blended gasoline SI engine: A sustainable transition

Muhammad Nasir Bashir [a], Muhammad Usman [b], Fahid Riaz [c], Touqeer Ahmad [b], Yasser Fouad [d], M. Shameer Basha [e], Muhammad Mujtaba Abbas [b], Joon Sang Lee [a,*]

[a] *Department of Mechanical Engineering Yonsei University, Seoul, 120-749, Republic of Korea*
[b] *Department of Mechanical Engineering, University of Engineering and Technology, GT Road, Lahore, 54890, Pakistan*
[c] *College of Engineering, Abu Dhabi University, Abu Dhabi, United Arab Emirates*
[d] *Department of Applied Mechanical Engineering, College of Applied Engineering, Muzahimiyah Branch, King Saud University, P.O. Box 800, Riyadh, 11421, Saudi Arabia*
[e] *Department of Mechanical Engineering, College of Engineering, Qassim University, Buraydah, 51452, Saudi Arabia*

GRAPHICAL ABSTRACT

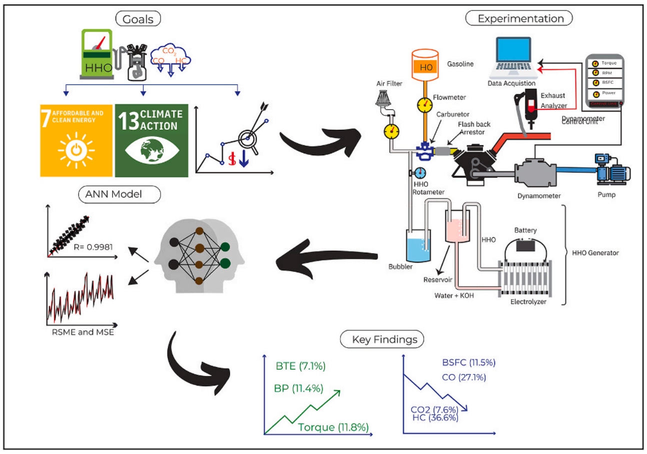

* Corresponding author.
E-mail address: joonlee@yonsei.ac.kr (J.S. Lee).

https://doi.org/10.1016/j.csite.2024.105562
Received 8 June 2024; Received in revised form 21 November 2024; Accepted 24 November 2024
Available online 26 November 2024

A R T I C L E I N F O

Keywords:
Artificial neural network (ANN)
Hydrogen blends
Internal combustion (IC) engines
Emission reduction
Engine optimization

A B S T R A C T

In striving for sustainable alternatives to gasoline, Oxyhydrogen (HHO) has emerged as a promising substitute for Internal Combustion Engines (ICEs). HHO blends not only improve engine efficiency but also reduce harmful emissions. On-site, HHO utilization in the engine, eradicates low energy density and storage challenges. The current study combined cutting-edge machine learning (ML) techniques like Artificial Neural Network (ANN) and Gradient-based optimization to effectively utilize HHO with gasoline. Experimentation involved a single-cylinder spark ignition (SI) engine fueled by varying HHO-gasoline blends across different loads and speeds. Iterative tuning of the loss function led to the identification of the optimal architecture, denoted as 2HL-10N (2 hidden layers with 10 neurons each), with impressive correlation coefficients (0.99481 for training, 0.9781 for validation, 0.96914 for testing, and overall, 0.98819). Subsequently, ANN led Gradient-based optimization unveiled key performance metrics along with emissions. Upon implementing optimized conditions (HHO: 3.78 l/m, load: 100 %, and 3465 rpm), notable enhancements were observed. The torque and efficiency increased by 11.8 %, and 7.1 %, respectively. Furthermore, brake-specific fuel consumption, carbon monoxide, and hydrocarbon emissions showed a reduction of 11.5 %, 27.1 %, and 36.6 %, respectively. ANN based optimal engine operation revealed HHO as a potential replacement for conventional gasoline.

1. Introduction

Modern transportation heavily relies on ICEs. Over 99.9 % of global vehicles, including 1.4 billion cars and 380 million commercial vehicles, utilize ICEs, with further growth anticipated [1]. ICEs utilizing fossil fuels account for 25 % of the world's power and, as a consequence, generate about 10 % of the world's greenhouse gas (GHG) emissions [2]. Industrial expansion and rapid population growth accelerate the use of conventional fuels, threatening the environment, energy security, and economic stability [3,4]. The shift to new technologies is promising, but the intricate shift requires consideration of infrastructure, economy, and society's complexities.

United Nations, in 2015, developed sustainable development goals (SDGs) to tackle such complexities [5]. Consequently, the significance of ICEs powered by alternative fuels such as hydrogen grows exponentially [6–8]. Various studies focused on different SDGs for better operation of the engines. The various projects linked to SDG 7 were performed to enable access to sustainable, reliable, affordable, and modern energy for all. Furthermore, the impact of energy utilization on the environment was also studied to take action against climate change and to promote environment-friendly technologies for global climate action (SDG 13) [9,10].

Hydrogen usage in traditional gasoline engines improves engine power and torque. Additionally, it decreases the harmful exhaust gases [11]. However, the inherent drawbacks of hydrogen like low energy density and high flame temperature, cause a reduction in the engine power along with higher levels of oxides of nitrogen (NOx). Challenges like distribution networks, and costly production and storage of hydrogen, hindered widespread hydrogen engine adoption [12,13].

Comparatively, hydrogen-blended conventional engines improve combustion duration and reduce emissions over mono-fuel engines by utilizing surrogate energy sources like methanol, ethanol, and methane [14]. Furthermore, Hydrogen's quicker flame and ample oxygen requirement boost engine efficiency [15]. Researchers are directing their efforts toward addressing the challenges of introducing HHO gas, an alternative manifestation of hydrogen. HHO acts as both a fuel carrier for hydrogen and a combustor that assists with oxygen. Due to its wide range of flammability, it can be used in ICEs as a gaseous fuel similar to hydrogen. In addition, it

Table 1
Nomenclature.

Parameters	Abbreviation
AAD	Average Absolute Deviation
ANN	Artificial neural networks
BP	Brake Power
BSFC	Brake Specific Fuel Consumption
BTE	Thermal Efficiency
CO_2	Carbon dioxide
CO	Carbon monoxide
HC	Hydrocarbons
HHO	Oxyhydrogen
ICE	Internal Combustion Engine
MAE	Mean Average Error
NOx	Nitrogen Oxide
RMSE	Root Mean-Square-Error
R^2	Coefficient of Determination
RSM	Response Surface Methodology
SEP	Standard Error of Prediction

Table 2
An overview of the impact of hydroxy gas utilization in spark ignition engines.

Author(s)	Fuel(s) used	BP	BSFC	BTE	CO	CO_2	HC	NOx	ANN
Nabil & Khairat [30]	Gasoline + HHO	↑	↓	↑	↓	×	↓	×	×
Wang et al. [31]	Gasoline + 2 % and 4 % of HHO as the total intake mixture.	×	×	↑	↓	×	↓	↑	×
Falahat et al. [26]	Gasoline + HHO	↑	×	↑	↓	×	×	↓	×
Al-Rousan [32]	Gasoline + HHO as Supplementary Fuel	×	↓	↑	×	×	×	×	×
Patil et al. [33]	Gasoline + HHO	×	↓	↑	×	×	×	×	×
Wang et al. [24]	Gasoline + HHO as Supplementary Fuel	↑	↓	↑	↓	×	↓	↑	×
Sa'ed & Al-Rousan [34]	Gasoline + HHO was introduced before the carburetor's downstream	×	↓	×	↓	×	×	↓	×
Krishna et al. [35]	Gasoline + HHO	×	×	↑	↓	×	↓	↓	×
Karagöz et al. [36]	(a) 3.75 % (2.5 % H_2 + 1.25 % O_2) (b) 7.5 % (5 % H_2 + 2.5 % O_2)	↑	↓	↑	↓	×	↓	↑	×
Mohan et al. [26]	Gasoline + HHO	×	×	↑	↓	×	↓	↑	×
Al-Rousan & Musmar [37]	Gasoline + HHO through Air Injection	↑	↓	↑	↓	×	↓	↑	×
Krishna [38]	Gasoline + HHO	↑	↓	↑	↓	×	×	↓	×
Wang et al. [39]	Gasoline + H_2 and O_2 are introduced separately to the engine.	↑	↓	↑	↓	×	↓	↑	×
Al-Rousan et al. [40]	Gasoline + HHO was introduced before the carburetor's downstream	×	×	×	↓	↓	×	↓	×
Zhao et al. [41]	a) Gasoline port injection + HHO b) Gasoline direct injection + HHO	↑	↓	↑	↓	×	↓	↑	×
Karagöz et al. [42]	Gasoline + HHO	↑	↓	↑	↓	×	↓	↑	×
Le Anh et al. [43]	The injection of gasoline and HHO downstream of the carburetor via an injector.	↑	↓	↑	↑	↑	↑	↑	×
El-Kassaby et al. [44]	Gasoline + HHO	↑	↓	↑	↓	×	↓	↓	×
Gutarevych et al. [45]	Gasoline + HHO was introduced before the carburetor's downstream	↑	↓	↑	×	×	×	×	×
Aminy et al. [46]	Gasoline + HHO introduced into the intake manifold as supplementary fuel	↑	×	×	↓	×	↓	×	×

" ↑" indicates an increase, "↓" denotes a decrease, and "×" indicates that the parameter wasn't studied.

can be used in a variety of air-fuel ratios due to its versatility [16]. HHO gas remarkable diffusivity promotes homogeneous fuel-air amalgamation and diffuses leaks quickly to prevent or mitigate dangers [16–18]. Oxyhydrogen can be prepared in number of ways, including electrolysis, thermolysis, steam methane reforming (SMR), etc. [19–21]. Among these, electrolysis is preferred the most because of its simplicity, low energy consumption, cutting-edge cost, reliability, durability, safety, and the potential to yield 99.98 % pure hydrogen [22,23].

However, low HHO density affects energy and fuel efficiency by increasing the demand for storage. High backfire risk due to short quenching distance can be reduced with a flame arrester. The presence of hydrogen content in HHO raises flame speed, demanding safer use in ICEs (see Table 1). Wang et al. examined SI engine performance using a gasoline and HHO mixture. The study concluded that raising HHO concentration enhanced brake thermal efficiency (BTE) by 6.9 %. Also, NOx emissions increased due to elevated combustion chamber temperature [24]. El-Kassaby et al. [25] found that adding HHO gas to the air/fuel mixture in an SI gasoline engine enhanced BTE by 10 %, cutting fuel consumption by up to 34 %. Additionally, emissions of carbon monoxide (CO), and hydrocarbons (HC) decreased by 18 %, and 14 %, respectively. Falahat et al. [26] enhanced gasoline engine efficiency with hydrogen enrichment, achieving a remarkable 23 % peak improvement in BTE. Torque and brake power (BP) also surged by 12.6 %, while brake-specific fuel consumption (BSFC) reduced by 16.9 %. Moreover, higher HHO gas flow rates led to decreased CO emissions. Krishna et al. [27] demonstrated a 14.8 % decrease in BSFC and a remarkable 17.5 % improvement in BTE using gasoline and hydroxy gas. In addition, HC and CO emissions declined by 31 % and 13 %, respectively. In another study, Shinagawa et al. [28] discussed how electrolytes directly take part in the reaction and affect electrode stability. Then, it was declared that the properly chosen electrolyte was a key factor in determining gas purity and crucial for the stability and activity of the electrocatalysts [29].

Table 2 summarizes prior studies by different researchers who utilized HHO in SI engines, aiming to enhance operational parameters. Conventional approaches to enhance hydrogen-blended ICEs, targeting emissions and performance issues, required expensive, time-intensive experimentation. Therefore, finding alternative strategies is crucial for sustainable practices. Table 2 highlights a noticeable gap in the research, as the existing studies have not yet harnessed the potential of Artificial Intelligence (AI) driven modeling techniques.

Several practices involving artificial neural networks (ANN), support vector regression, random forest, and gradient regression tress are used for optimization and prediction [46]. However, computational modeling, like ANN and Gradient-based optimization has risen to predict and optimize ICE features (combustion, emissions, and performance) via diverse input settings to mitigate the need for resource-intensive experimentation. Fu et al. [47] employed an ANN algorithm to predict the efficiency of an SI engine powered with gasoline. Comparisons between actual data and predictions revealed a well-trained network's accurate forecasts with minimal RMSE. Moreover, a study conducted by Liu et al. [48] suggested that ANNs had better learning capability than support vector regression. Similarly, a study conducted by Liu et al. [49] utilized ANN to forecast the performance, combustion phasing, and emissions of a natural gas-powered SI engine. Huang et al. [50] used ANN to accurately predict various engine responses and proved ANN a suitable tool for engine analysis. Sun et al. [51] created ANN based models using Levenberg-Marquardt, Bayesian regularization, and scaled conjugate gradient algorithms to forecast torque, NOx, CO, HC, and particulate number (PN). The models exhibited excellent fitting and prediction, with a correlation coefficient of 0.99. Samuel et al. [52] used ANNs to model and predict the production of biofuel from

Table 3
Specification of HHO generator.

Specification	Details
Plate Material	SS 316-L
Size (cm)	$16.5 \times 0.1 \times 16.5$
No. of plates	24
Electrodes	Anode plates at centre (2), Cathode plates on ends (2)
Plates space (mm)	2
Input (A, V)	0–60, 35
Catalyst	KOH in distilled water
HHO generation (SCFH)	0–10

Table 4
Technical aspects of the test engine.

Specification	Value
Bore x stroke	68×45 mm
Displacement	163 cm^3
Compression ratio	8.5:1
Number of valves	2
Fuel tank capacity	3.1 L
Lubricating oil storage	0.6 L
Power	3.6 kW

tobacco seed oil. The studies conducted earlier revealed the performance improvement of engines when used with HHO in blended form due to oxygen content and calorific value [53–55].

Table 2 highlights the absence of AI-oriented approaches in the domain of modernization of research methodologies in line with the advancements of the AI era. ANN aptitude to understand complicated arrangements and interactions of data, delivers viable solutions in automation and decision making. This research introduces an innovative solution for tackling the issues related to hydrogen-blended ICEs by employing the capabilities of AI, which is an uncharted domain. A viable and novel strategy is presented for enhancing engine efficiency, curbing emissions, and addressing worldwide climate challenges sustainably by integrating two sophisticated ML techniques (ANN and Gradient-based optimization). A grounding path opens up that has the potential to transform the field of sustainable transportation by synergizing AI-driven techniques with ICEs. The study aims to achieve the targets of two sustainable development goals (7 and 13), which highlight the significance of clean energy and climate action. The integration of two cutting-edge ML techniques contributes significantly to global environmental preservation, and energy conservation efforts by reducing resource-intensive experimentation. Also, this work frames as an encouragement for greener paths of the transition phase of automotive industry.

2. Materials and methods

2.1. Experimental setup and test plan

A small cell electrolyzer composed of stainless-steel plates (SS316L) was created to develop HHO from distilled water. The specifications of HHO generator are shown in Table 3. Potassium Hydroxide (KOH) was used as the catalyst together with distilled water at a concentration of 6 g/L (mass by volume) owing to its enhancement in conductivity and inhibition of corrosion. The low-cost structure of the cell in comparison to that of the wet cells makes it ideal for power and automobile usage. Additionally, the cell possesses good electrical conductivity, good corrosion resistance, high melting point, low weight and excellent thermal conductivity. SS316L is used as the cell's electrode, thereby helping to increase electrolysis efficiency. A reservoir or separation tank supplied electrolyte (water and KOH) to the cell ensuring continuous HHO production. A ball valve adds catalyst-containing distilled water. Generated HHO along with water droplets return to the tank's top. Hoses manage water inflow and HHO gas outflow from the cell. HHO gas is then sent to the carburetor upstream. Eqs. (1)–(3) [56] demonstrate HHO production process of the electrolyzer.

$$\text{At cathode}: 4H_2O(l) + 4e^- \rightarrow 2\,H_2(g) + 4OH^-(aq) \tag{1}$$

$$\text{At anode}: 4OH^-(aq) \rightarrow O_2 + 2H_2O(l) + 4e^- \tag{2}$$

$$\text{Overall reaction}: 2H_2O(l) \rightarrow 2H_2(g) + O_2(g) \tag{3}$$

An air-cooled, single-cylinder, four-stroke, spark-ignition HONDA GP160 engine was employed without any alteration in the study for testing purposes. The technical aspects of the test engine are detailed in Table 4. A Dynomite seven-inch water brake dynamometer was utilized for performance testing. A water pump and a system of pipes were used to manage the hydraulic load. The control panel of the Dynomite recorded speed, torque, and BP. Gasoline consumption was measured using a flowmeter. The hydroxy gas flow rate was measured using a gas rotameter in standard cubic feet per hour (SCFH). Brake specific fuel consumption (BSFC) and BTE were

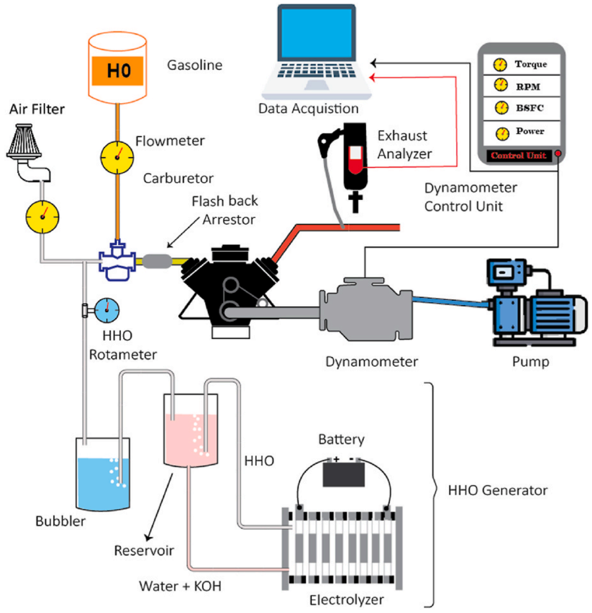

Fig. 1. Schematic of experimental set up.

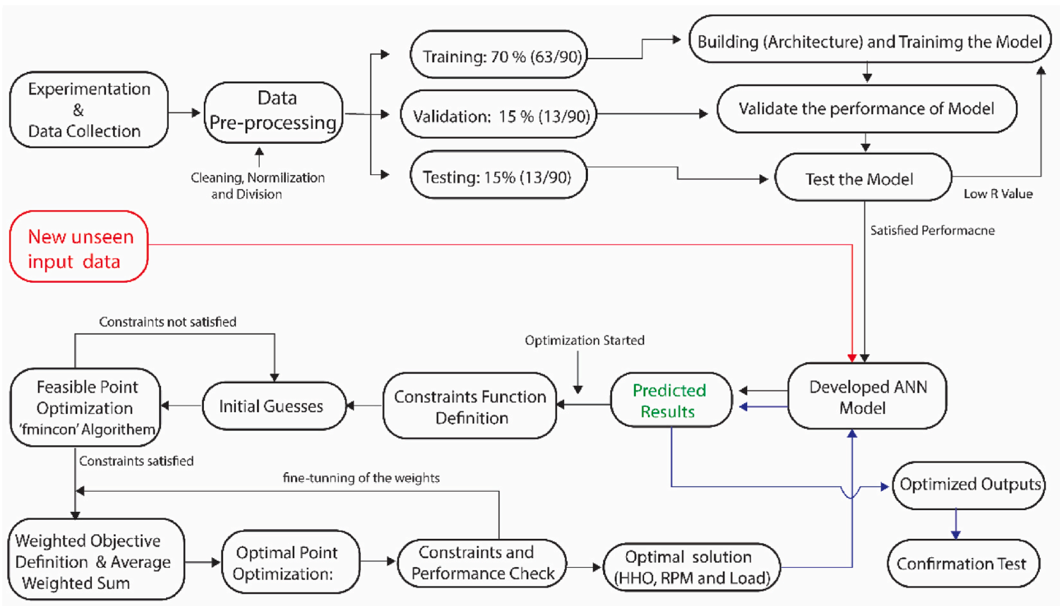

Fig. 2. Flow chart for ANN integrated optimization model.

determined based on density and heating values. The emissions were quantified using EMS-5002 exhaust analyzer.

Fig. 1 illustrates the experimental setup. HHO was used with gasoline in concentrations of 0, 2, 4, 6, and 8 standard cubic feet per hour (SCFH), equivalent to 0, 0.94, 1.89, 2.83, and 3.78 l/min. The gas was supplied to the system by connecting the HHO cell to the upstream of the carburetor. The fuel mixtures were labeled as H0, H2, H3, H4, H6, and H8. The engine's rotational speed was systematically enhanced from 1300 to 3700 revolution per minute in enlargements of 300 rpm. Two different load conditions of 50 % and 100 % were also applied. Measurements were taken when the engine reached a stable operating state. H0 concentrations were used as a baseline for comparison with the other fuel blends. To ensure accuracy, each test was conducted three times, and the average outcomes were recorded. Due to the high combustibility of HHO gas, safety precautions are essential. A flashback arrester was installed as a precaution to stop gas from going back into the generator and igniting it. The HHO unit was operated only when the engine was running. The leakages were eliminated by careful examination of the hose connections.

Table 5
Formulas to check the correctness of models.

Parameter	Mathematical Formulas
MSE	$\frac{1}{n}\sum_{i=1}^{n}\left(Y_{observed} - Y_{Predicted}\right)^2$
RMSE	$\sqrt{MSE}$
R^2	$1 - \frac{\sum\left(Y_{true} - Y_{Pridicted}\right)^2}{\sum\left(Y_{true} - y\right)^2}$

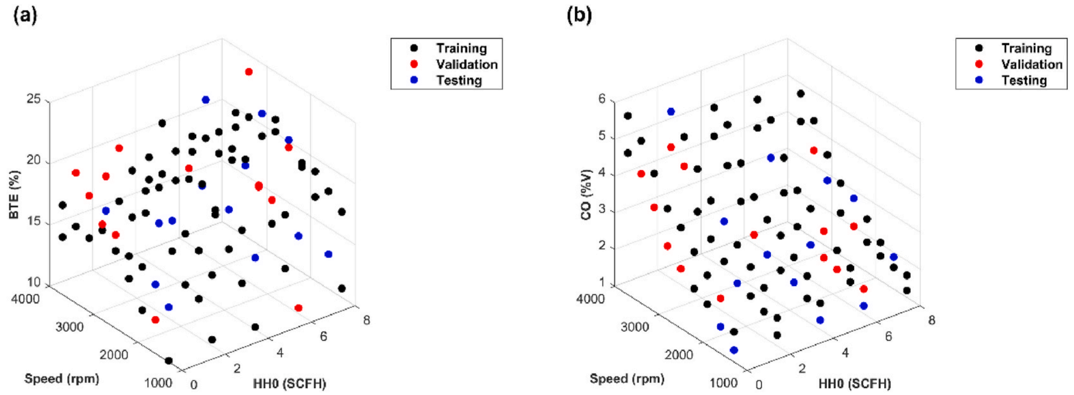

Fig. 3. Random distribution of data: (a) BTE; (b) CO.

Table 6
Design parameters of ANN models.

Specifications	Description
Software	MATLAB
Normalization Function	Zscore
Training Function	Trainlm
Training Algorithm	Levenberg-Marquardt
Activation Function	ReLU
Epochs	1000
In-Training Performance	Error histograms and regression plot
Post-training performance	R, MRE, and RMSE
Data	70 % (63/90) for training, 15 % (13/90) for testing, and 15 % (13/90) for validation
Stopping Criteria	Minimization of MSE

2.2. Development of ANN prediction model

Utilizing AI-based engine modeling presents a promising avenue for swiftly constructing adaptive models of intricate systems [57, 58]. These models showcase a remarkable capacity to handle data uncertainty while maintaining computational efficiency [59]. As a result, these models are well-suited for real-time prediction and interpolation tasks in control scenarios. Specifically, ANN possesses inherent adaptability, allowing for the creation of robust models that authentically replicate engine behavior across diverse studied variables. ANN's are inspired by biological neural systems and widely adapted. They are computational and mathematical tools employed to predict the performance and emission characteristics of engines [60]. ANNs typically consist of 3 layers: input, hidden, and output. Data is processed in the hidden layer, and predictions are made in the output (Fig. 2). The model undergoes training, testing, and validation. Metrics like regression coefficient, MRE, and RMSE assess the model's validation. Table 5 encompasses the formulas for the calculations of MSE, RMSE, and R^2 [61,62]. In the current work, MATLAB software was utilized for the development of the ANN prediction model. A total of 11 parameters were under examination. Among these, three variables, namely, HHO concentration, load, and RPM, were selected as input factors for the model. Meanwhile, the remaining eight parameters, including BP, BSFC, BTE, CO, CO_2, HC, and NOx, were designated as the model's output variables. To balance input features, promoting effective weight adjustments and faster learning in the ANN model, the 'zscore' normalization was employed. Weights serve as a long-term memory mechanism. The process of learning in an ANN involves iterative adjustment of these weights [63]. The study utilized 90 data sets each consisting of 3 input nodes and 8 corresponding outputs, resulting in a total neural data point for the output in the neural network. The 'divideind' function was used to split the data into three sets: 70 % for training, 15 % for validation, and 15 % for testing. This allowed for the randomized sampling of data points. To ensure a fair assessment of the model's functioning and generalizability, the data must

Table 7
Objective weights for engine performance optimization.

Variable	Torque	BP	BSFC	BTE	CO	CO_2	HC	NOx
Weight	1	1	−1	1	−1	−1	−1	−1
Objective	Maximize	Maximize	Minimize	Maximize	Minimize	Minimize	Minimize	Minimize

Table 8
Range and accuracy for recorded variables.

Measured parameters	Range	Accuracy	Uncertainty (%)
BP	0–50 kW	±0.05 kW	±1
Speed	0–8000 rpm	±5 rpm	±0.5
NO_x	0–5000 ppm	±1 ppm	±1
Fuel consumption	0–500 mL	±0.1 mL	±0.5
HC	0–5000 ppm	±1 ppm	±1
CO_2	0–18 %	±0.1 %	±1
CO	0–18 %	±0.01 %	±1

be systematically dissented into sets.

Fig. 3 shows the random distribution of torque and CO_2 data set. The training process utilized the 'trainlm' function, which involved the application of the Levenberg-Marquardt algorithm. This algorithm proves advantageous in managing non-linear challenges and achieving swift convergence, as it combines the strengths of both the Gauss-Newton and gradient descent techniques. The activation function chosen was Rectified Linear Unit (ReLU), although sigmoid and tanh functions are likewise frequently employed for analogous tasks [47,64]. To quantify the prediction error, the loss function was engaged. Subsequently, the error was transmitted in reverse via the system using backpropagation algorithm, leading to the adjustment of weights and biases. The adjustments were determined by evaluating the gradient of the loss function regarding the considerations. The modified weights and biases were subsequently revised in each iteration through the utilization of the 'Adam' optimization algorithm. The RMS prop method is also widely recognized in this context [65]. The network architecture was chosen, and iterations of the ANN model were executed based on the loss function and termination criteria outlined in Table 6 using the dataset.

The MSE criterion was adopted as the loss function to minimize during the search for the architecture. To prevent overfitting, the training of the network was stopped when the validation error began to rise. The evaluation of performance metrics, including R, MSE, and RMSE, facilitated the measurement of the models' stability and accuracy.

2.3. Development of gradient-based optimization model

The optimization is carried out using the 'fmincon' function, which is a gradient-based optimization technique capable of handling constrained nonlinear optimization problems. The optimization options are configured to display the iterative process and utilize the Sequential Quadratic Programming (SQP) algorithm for efficiency. The goal of the study was to optimize engine operation by adjusting the HHO concentration, load, and speed parameters (see Fig. 2) while considering constraints related to emissions (CO, CO_2, HC, NOx). An initial feasible point was determined by performing an optimization with a zero objective function while considering the constraints. The feasible point was then utilized as the initial point for the main optimization task. The objective function to be minimized was defined as a weighted sum of various predicted engine performance metrics, including Torque, BSFC, BTE, BP, CO_2, CO, NOx, and HC. The weights assigned to each metric are modifiable based on their priorities, allowing for customization according to specific optimization goals. Then, the assigned weights were chosen to balance engine performance metrics prioritizing torque, BP, BTE, maximization while minimizing emissions (see Table 7). The engine performance metrics were normalized using the 'Z-Score' method to ensure fair comparison across different scales. The normalized metrics were then combined using the predefined weights to calculate a weighted sum for each data point. The final optimization objective was to minimize the average weighted sum across all data points, thereby optimizing the engine's performance while taking into account the specified constraints. The constraints were defined using specific values for CO, CO_2, HC, and NOx emissions. In addition, the constraints were used to guide the optimization process and ensure that the resultant engine operation aligned with environmental regulations [66].

2.4. Uncertainty analysis

The analysis of uncertainties directs the correctness of recorded variables along with the extent of error related to the experimental data. Table 8 presents the range, accuracy and uncertainty associated with the recorded variables. Moreover, the total uncertainty was calculated using Eq. (4) [67]. The performance of the system was found to be accurate as the total uncertainty was 2.35 %.

$$Total\ Uncertainty = \sqrt{(U_{BP})^2 + \left(U_{Speed}\right)^2 + (U_{NOx})^2 + (U_{FC})^2 + (U_{HC})^2 + (U_{CO_2})^2 + (U_{CO})^2} \tag{4}$$

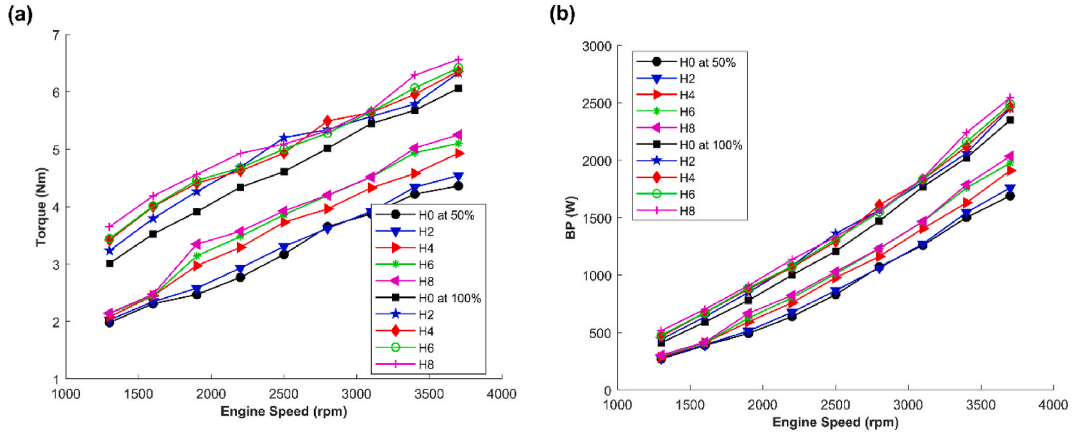

Fig. 4. Effect of HHO concentrations and engine speeds on output parameters: (a) torque; (b) BP.

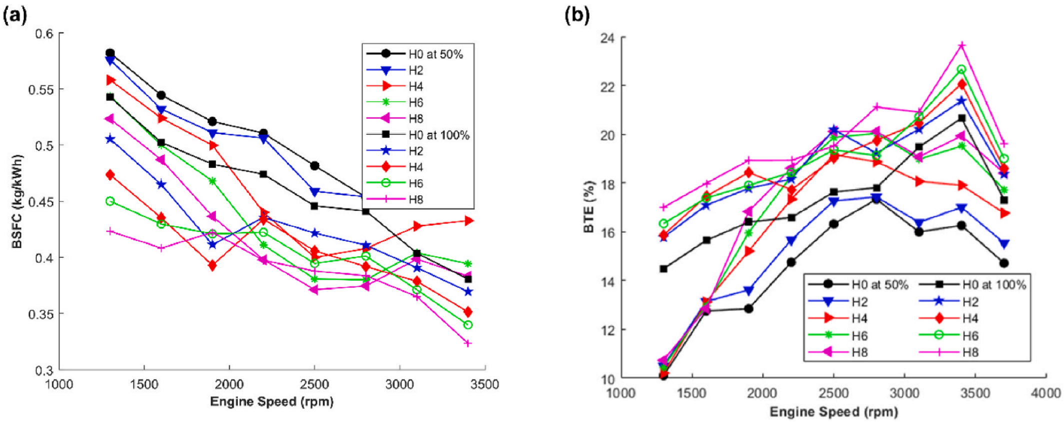

Fig. 5. Effect of HHO concentrations and engine speeds on output parameters: (a) BSFC; (b) BTE.

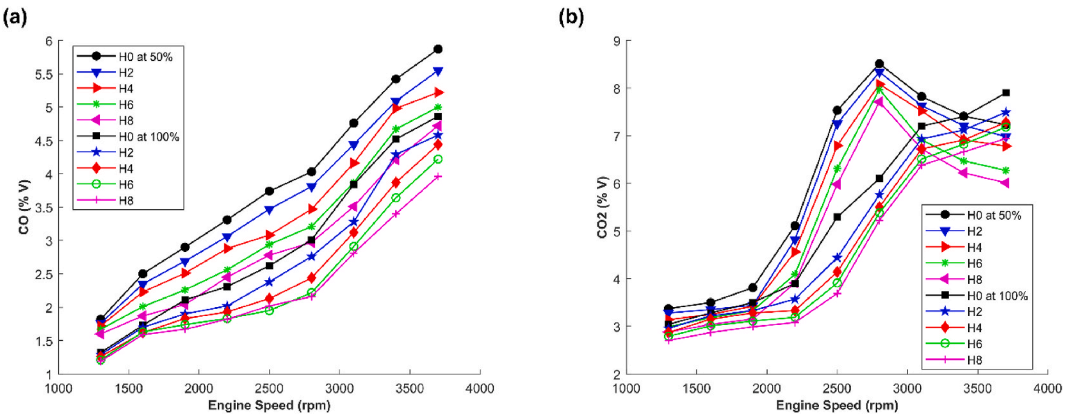

Fig. 6. Effect of HHO concentrations and engine speeds on output parameters: (a) CO; (b) CO_2.

$$Total\ Uncertainty = \sqrt{(1)^2 + (0.5)^2 + (1)^2 + (0.5)^2 + (1)^2 + (1)^2 + (1)^2}$$

$$Total\ Uncertainty = 2.35\%$$

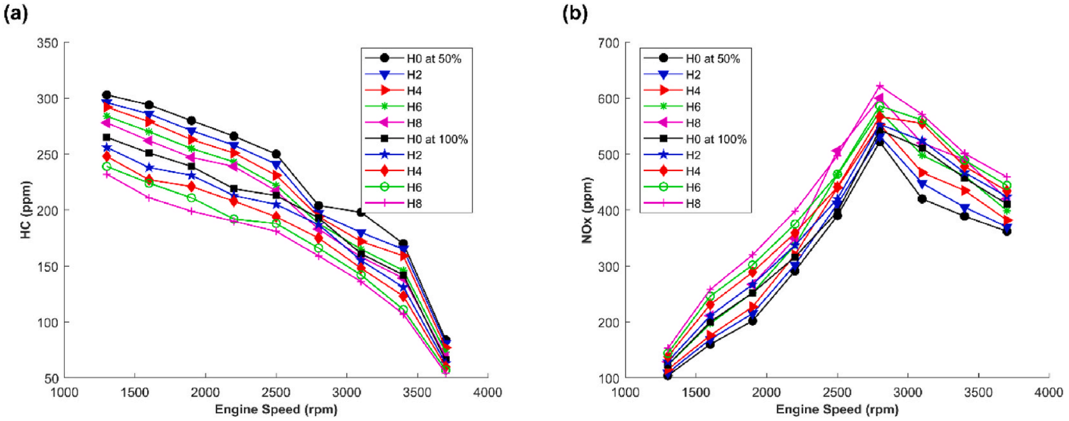

Fig. 7. Effect of HHO concentrations and engine speeds on output parameters: (a) HC; (b) NOx.

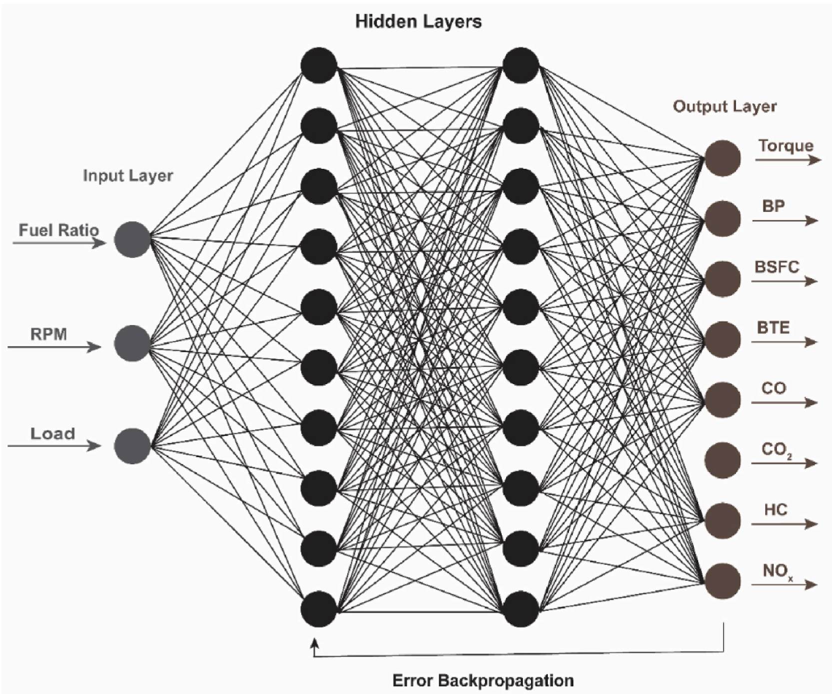

Fig. 8. The architecture of 2HL-10N prediction model.

3. Results and discussion

3.1. Performance and emissions

The relationship between torque and engine speed is presented in Fig. 4(a) for different HHO concentrations, encompassing both 50 % and 100 % load conditions. The study conducted by Falahat et al. [26] suggested 12.6 % increase in both torque and BP as hydrogen concentration raised, compared to the engine's performance when operating on H0. The torque increased by 2.8 %, 12.2 %, 17.4 %, and 19.6 % at a 50 % load condition and by 6.3 %, 7.8 %, 8.2 %, and 11.3 % at a 100 % load for H2, H4, H6, and H8 mixtures, respectively. Fig. 4(b) also indicates that a gradual increase in hydrogen significantly improved the BP of the engine. The average increase of 4.2 %, 9.5 %, 12.5 %, and 15.1 % were observed for the mixtures H2, H4, H6, and H8, respectively. The flame speed of general fuels like gasoline, CNG, and CNG-HHO blend are 0.5, 0.41 and 1.85, respectively [53]. However, the exponential rise in HHO's heating value, owing to two hydrogen atoms per unit, demands more combustion energy. Higher HHO concentration intensifies energy release due to hydrogen's flammability, lessening the need for additional combustion. Elevated pressure generation in the engine cylinder enhances torque output across the speed range [26,36].

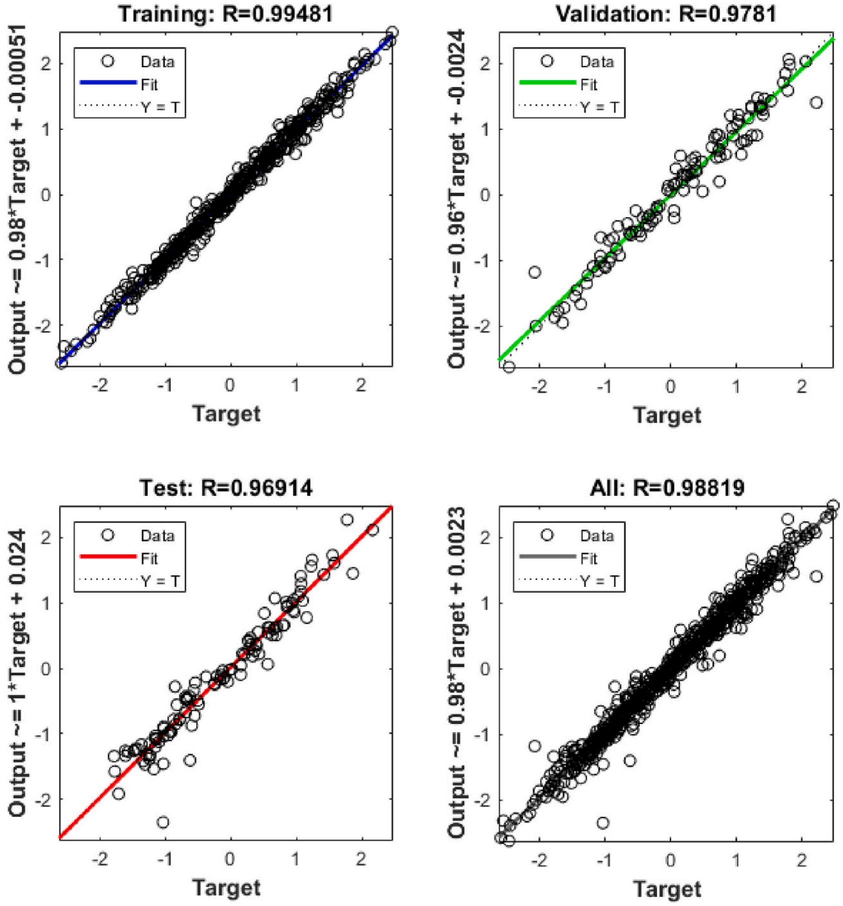

Fig. 9. Regression plot of 2HL-10N model.

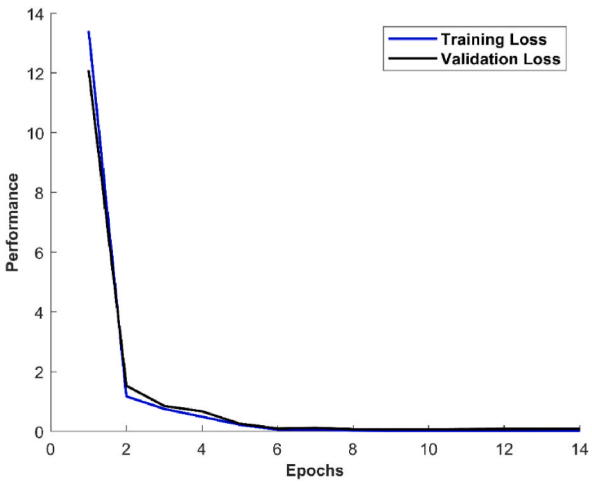

Fig. 10. Learning Curve of 2HL-10N model.

It is clear from Fig. 5(a) that BSFC continually reduces as the concentration of HHO rises, which can be ascertained from the literature [26,35], showing 14.8 % and 16.9 % decline, respectively. Average BSFC declined by 2.4 %, 9.8 %, 14.9 %, 17.7 % at 50 % load and 7.0 %, 10.8 %, 11.9 %, 15.2 % at 100 % load conditions for H2, H4, H6, and H8 blends, respectively. It is credited to the quicker burning of hydrogen which follows a constant volume process. Consequently, higher power is generated from the energy

Table 9
Performance metrics of the 2HL-10N model for each output (training set).

Parameter	R	MRE	RMSE
Torque	0.99792	−0.2208	0.0633
BP	0.99881	−0.0004	0.0484
BSFC	0.98896	−0.7270	0.1427
BTE	0.99002	−0.0291	0.1359
CO	0.99776	−0.0372	0.0675
CO_2	0.99708	0.0463	0.0778
HC	0.99474	0.1253	0.1055
NOx	0.99233	0.0424	0.1223

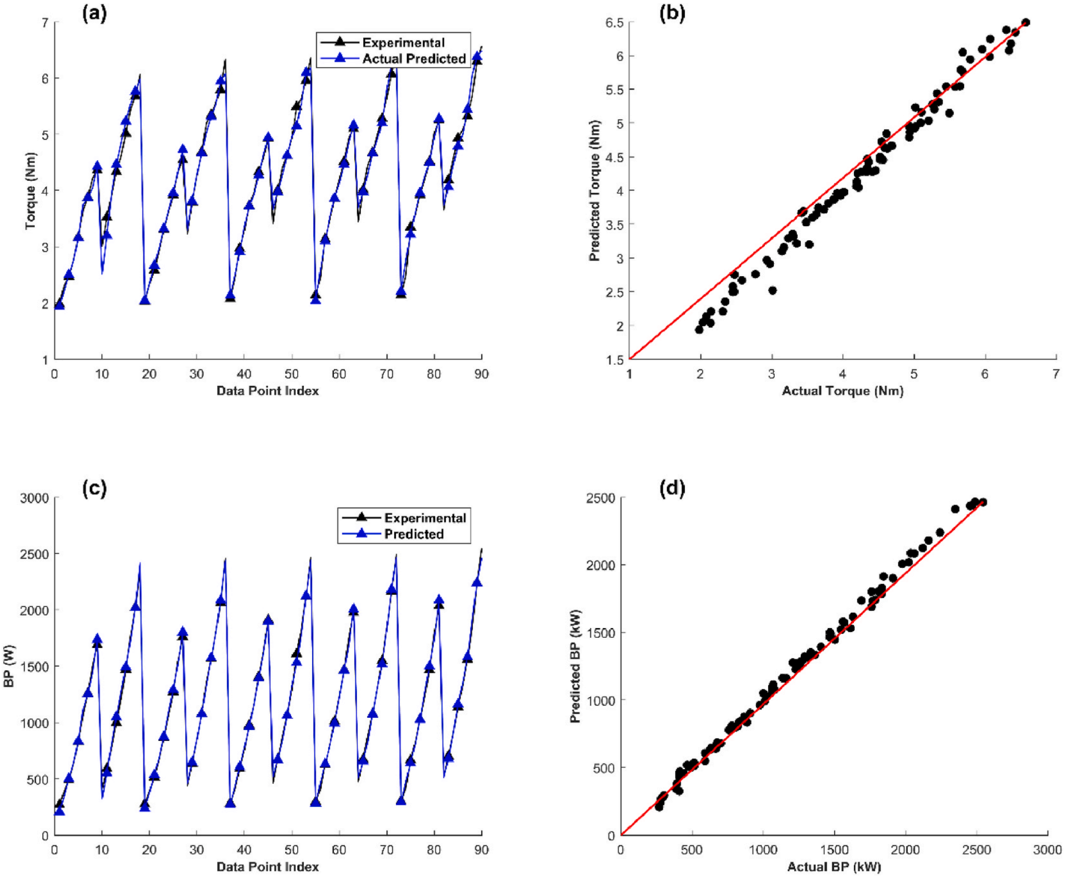

Fig. 11. Comparative analysis of various data sets: (a) torque with data point index; (b) actual and predicted torque; (c) BP with data point index; d) actual and predicted BP.

delivered to the engine. Furthermore, the addition of oxygen to the mixture enhances burning process [22]. In Fig. 5(b), the increase in the BTE can be observed for H2, H4, H6, and H8 as 4.2 %, 11.9 %, 17.3 %, 19.5 % at 50 % load and 7.8 %, 8.6 %, 9.6, 13.9 % for 100 % load condition, respectively. The literature revealed up to 17.5 % increase in BTE of the engine [24,26,27]. The stable hydrogen addition yields quicker, efficient combustion with a denser mixture, promoting lean burn. Oxygen improves combustion and increases engine thermal efficiency [54,55].

The addition of hydrogen in the engine reduces the overall carbon percentage and improves the hydrogen ratio which leads to smoother and lean combustion with better flame propagation and combustion velocities. The decrease in the carbon values significantly improves the emissions of the engine as most of the engine emissions are carbon oxides and unburnt hydrocarbons. The impacts of hydrogen addition on CO emissions are presented in Fig. 6(a), which are within the range as mentioned in the literature (31 % decline) [25,27]. The addition of hydrogen reduces CO emissions which could be apprehended by quick and complete oxygen consumption. CO emissions decreased by 7.1 %, 13 %, 18.4 %, and 22.8 % on average for H2, H4, H6, and H8 fuel blends, respectively. Similarly, emissions of CO_2 also declined by 3.7 %, 7.1 %, 12.5 %, and 16 % at 50 % load and 5.7 %, 9.3 %, 12 %, and 14.9 % at 100 % load for H2, H4, H6, and H8 blends respectively (Fig. 6(b)).

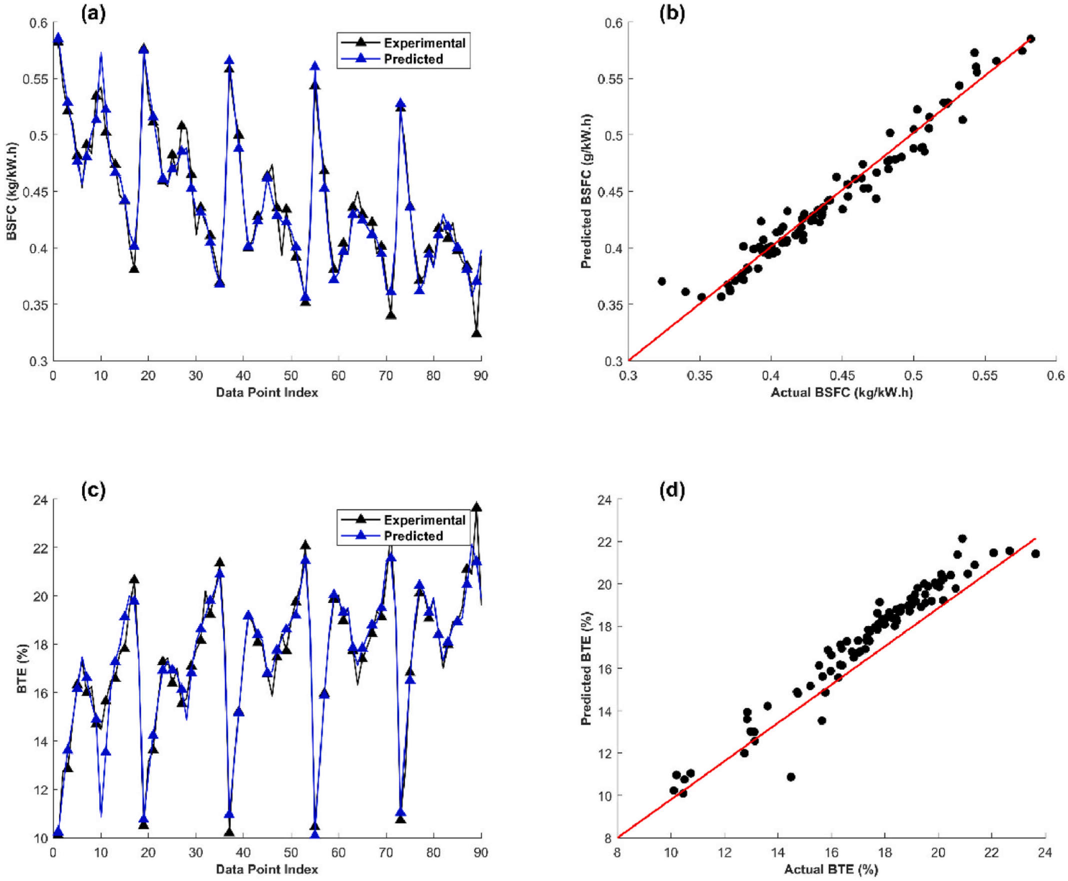

Fig. 12. Comparative analysis of various data sets: (a) BSFC with data point index; (b) actual and predicted BSFC; (c) BTE with data point index; d) actual and predicted BTE.

Fig. 7(a) depicts that for all combinations of fuel, HHO addition pointedly mitigated the HC emissions. The decrease in HC emissions was found to be 3.6 %, 6.4 %, 9.9 %, and 12.5 % at 50 % load and 4 %, 8.3 %, 12.5 %, and 16 % at 100 % load for H2, H4, H6, and H8 respectively. The unburnt HC was produced due to delayed flame development and propagation. The addition of hydrogen rectifies the mentioned problem by producing a denser mixture and reducing the flame propagation time, thus in return marginally decreasing the HC emissions [25,27]. The introduction of HHO produced a significant exception to the various other tailpipe emissions in the form of increased NOx emissions. It can be observed from Fig. 7(b) that NOx emission increases with the addition of HHO gas. The increments in NOx emissions were 4 %, 9.2 %, 14.5 %, and 20.3 % for blends of H2, H4, H6, and H8, respectively, which complimented the results of the study conducted by Wang et al. [24]. The emission of nitrogen oxides increases with the increase in the exhaust temperature as the tendency of nitrogen to form compounds is relatively high at elevated temperatures. The increased NOx emission with hydroxy gas blend is subjected to increased flame production and complete burning of fuel [39,41].

3.2. Effectiveness of ANN built prediction model

The neural network went through several iterations guided by the loss function and stopping criteria outlined in Table 6. The multilayer diagram (Fig. 8) of ANN involves fuel ratio, engine speed and load as three variables for input layer and BP, torque, BTE, BSFC, CO_2, HC, CO, and NOx as output with eight layers for performance and emissions characteristics of the engine. As a result, the optimized architecture for the ANN model was found to be 2 hidden layers with 11 neurons (2HL-11N).

The ANN network detected the forecast. The regression plot in Fig. 9 reveals that data points tend to group closely near a diagonal line. Notably, 2HL-10N model demonstrated robust performance with superior R values of 0.99481 for training, 0.9781 for validation, 0.96914 for testing, and an overall R-value of 0.98819.

Fig. 10 displays the learning curves, illustrating a noticeable initial training and validation loss. With the number of training and validation instances increased, the loss consistently decreased and levelled off. An effectively fitted model characterized by training and validation losses being close, with validation slightly higher. The result highlighted the importance of finding correct equilibrium concerning model intricacy and ability to extract patterns from data in a generalized manner. This balance helped avoid overfitting and underfitting, ultimately leading to improved performance. Table 9 shows the performance metrics of 2HL-10N model. The R, MRE and

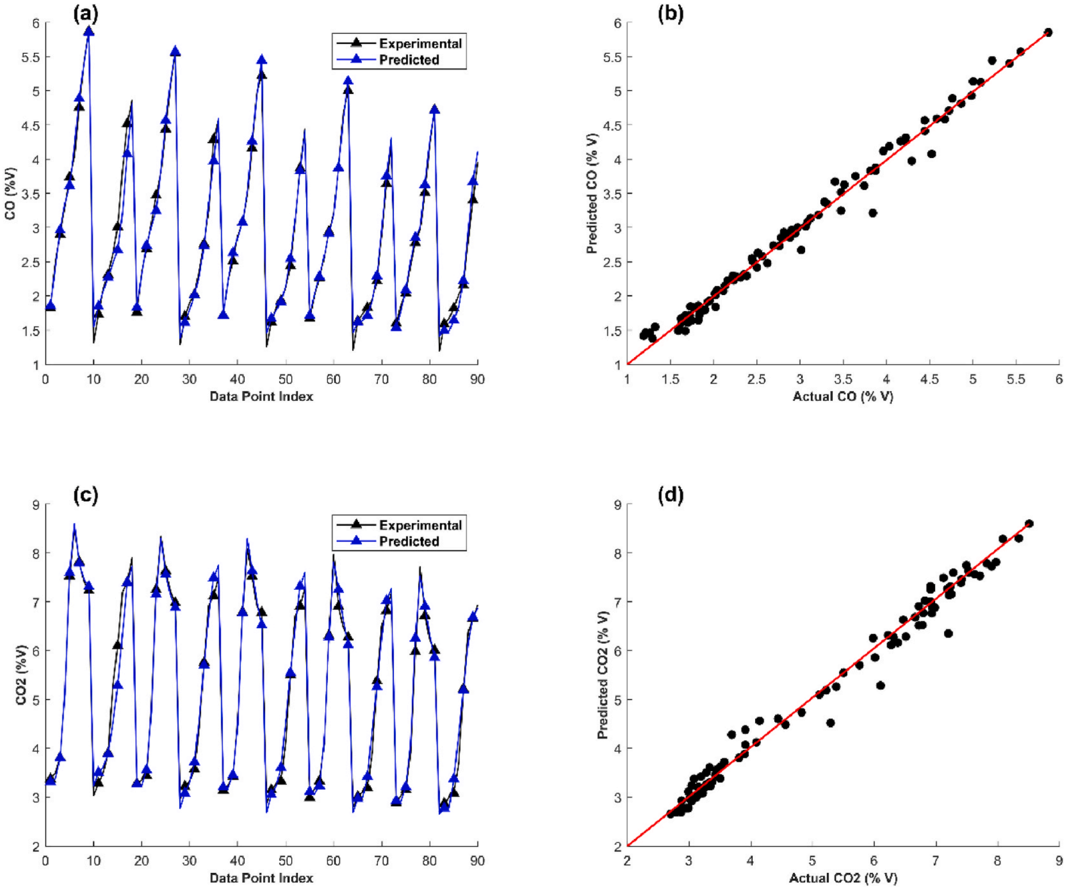

Fig. 13. Comparative analysis of various data sets: (a) CO with data point index; (b) actual and predicted CO; (c) CO_2 with data point index; d) actual and predicted CO_2.

RMSE values of all the outputs (brake power, torque, brake specific fuel consumption, brake thermal efficiency, carbon monoxide, carbon dioxide, unburnt hydrocarbon and oxides of nitrogen) used in training revealed acceptable performance of ANN network.

The model's performance and accuracy were comprehensively evaluated by plotting the predicted outputs against the experimental values. Fig. 11(a) reveals performance of variable torque, focusing on the alignment between predicted and experimental values at each data point index. These indices represent the sequence of data points in the dataset, each corresponding to a distinct experimental condition. Notably, Fig. 11(b) showcases the proximity of predicted and experimental torque values for each data point index, providing graphical validation of 2HL-10N model's performance metrics. Furthermore, Fig. 11(b) illustrates that the entire torque dataset forms a clustered distribution along a diagonal line at 45°. Similarly, Fig. 11(c) and (d) demonstrate analogous trends for BP. The evaluation of BSFC, BTE (Fig. 12), CO, CO_2 (Fig. 13), HC and NOx (Fig. 14) emissions depicted that the data was clustered around the line bisecting abscissa and ordinate axes at 45°. The predictive model captured trends and overall behavior quite well. The ANNs model found accurate in predicting various parameters of engines, including performance and emission. The model portrayed a strong alignment among predicted and experimental data for torque, BSFC, BTE, BP, along with CO_2, HC, CO, and NOx emissions. This consistent performance across different metrics highlights the model's reliability in forecasting both engine efficiency and emissions, reinforcing the model's effectiveness.

The model's robustness was comprehensively evaluated by plotting the test sets against the experimental values [67,68]. The coefficient correlation (R), and RMSE can be seen in Table 10. Most of the values revealed the higher effectiveness of the developed network.

Fig. 15 portrays a comparative analysis of tested and experimental torque. The R value for the torque is 0.97299 that implies significant alignment between the experimental and predicted outcomes. Subsequently, the developed model is appropriate for the estimation of engine torque. Accordingly, the predicted data ascertained from the developed model was compared with the experimental data for comparative analyses of BP (Fig. 16), CO (Fig. 17), and NOx (Fig. 18). The correlation coefficient (0.98451 and 0.95638 for BP and NOx respectively) and RMSE (0.11321 and 0.06149 for BP and NOx respectively) signify reliability of 2HL-10N Artificial Neural Network. The experimental and estimated values found in vicinity, revealing the superior effectiveness of the network. The case is not the same for CO as it has a lower correlation coefficient of 0.81927 but one can argue that it still has a predictive capability. Other parameters in the study have a low Mean Relative Error (MRE) except for BP which has a relatively high

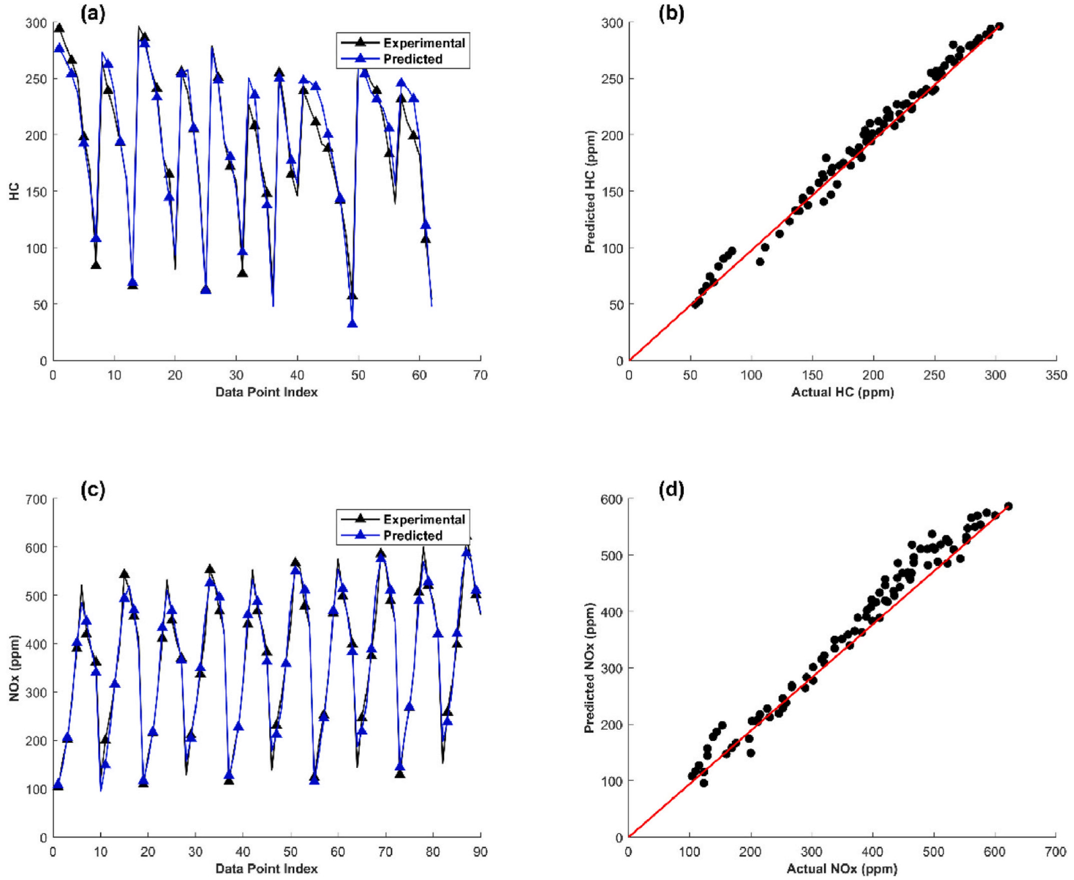

Fig. 14. Comparative analysis of various data sets: (a) HC with data point index; (b) actual and predicted HC; (c) NOx with data point index; d) actual and predicted NOx.

Table 10
Robustness metrics of model for the output (test set).

Parameters	R	RMSE
Torque	0.97299	0.054272
BP	0.98451	0.11321
CO	0.81927	0.10286
NOx	0.95638	0.061499

mean of 0.2422 showing how scattered values are within BP. The low RMSE values all further support the credibility of the model in making accurate and precise forecasts for practical applications in predicting engine behaviors.

3.3. Gradient-based optimization of engine

The optimal engine operational parameters were determined using gradient-based optimization in the context of artificial intelligence. These included a load configuration of 100 %, an HHO concentration of 8 SCFH, and an engine speed of 3465 rpm. After that, the trained ANN model was used to forecast output. The optimized outputs are listed in Table 11. An experimental verification was performed through a confirmation test to confirm the optimized results. The findings are also summarized in Table 11.

Running the engine using the identified parameters produced the most favorable outcomes, which were in line with the study's goals. Table 12 presents a comparison of the engine outputs when operating at 3465 rpm, 100 % load, and 8 SCFH HHO concentration. The same speed and load conditions were considered for the gasoline-fueled engine. Positive values in the table signify a percentage increase, while negative values indicate a percentage reduction.

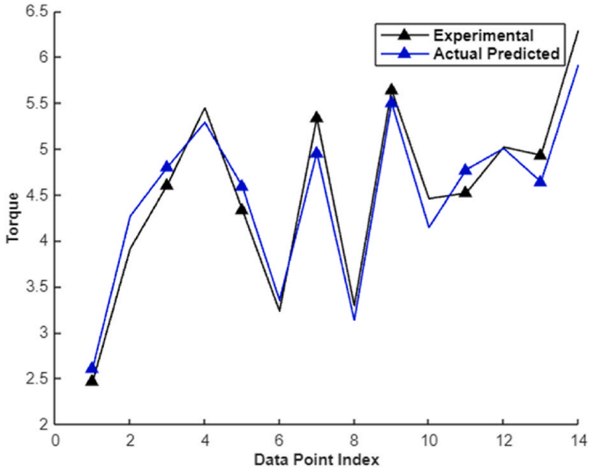

Fig. 15. Comparative analysis of tested and experimental torque.

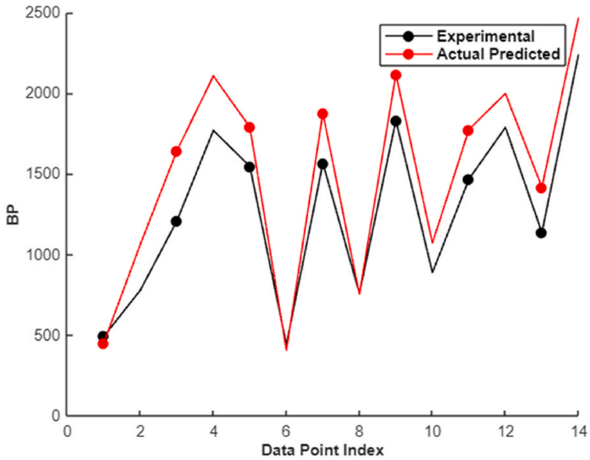

Fig. 16. Comparative analysis of tested and experimental BP.

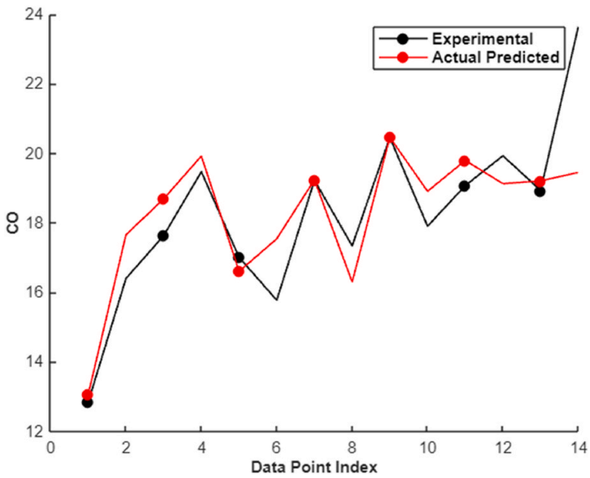

Fig. 17. Comparative analysis of tested and experimental CO.

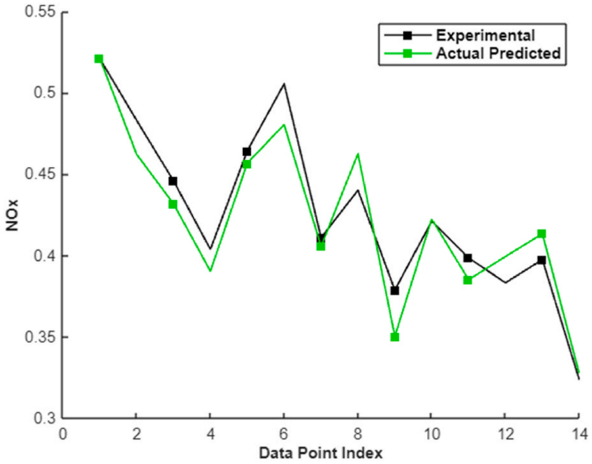

Fig. 18. Comparative analysis of tested and experimental NOx.

Table 11
Comparative evaluation of optimized outcomes and verification test results.

	Torque (Nm)	BP (W)	BSFC (Kg/kWh)	BTE (%)	CO (% V)	CO_2 (% V)	HC (ppm)	NOx (ppm)
Predicted- optimized values	6.35	2253	0.337	22.12	3.293	6.841	90.88	561.241
Experimental values	6.60	2334	0.353	23.07	3.469	7.166	95.45	592.009
% Error	3.8	3.6	4.5	4.1	5	4.5	4.8	5.2

Table 12
Comparative analysis of H8 blend and gasoline at optimal operating conditions.

HHO (SCFH)	Load (%)	RPM	Torque (Nm)	BP (kW)	BSFC (Kg/kWh)	BTE (%)	CO (% V)	CO_2 (% V)	HC (ppm)	NOx (ppm)
8	100	3465	6.35	2.25	0.337	22.1	3.29	6.84	90.88	561.2
0	100	3400	5.678	2.02	0.381	20.6	4.52	7.4	142	457
Percentage difference			11.8	11.4	−11.5	7.1	−27.1	−7.6	−36.0	22.8

4. Conclusion

Numerous investigations on hydrogen utilization with gasoline are available in the literature. The storage issue to supply hydrogen at the inlet of engine can be resolved via on board HHO gas production and utilization. The current work combined ANN and Gradient-based ML techniques to predict and optimize engine operation when fueled with gasoline and HHO blends. The work directly aligns with SDGs 7 and 13, contributing to the development of sustainable energy while simultaneously addressing climate change. The novel study revealed that with the increase in HHO concentration, BP, BTE and torque were increased. Furthermore, BSFC, CO, HC and CO_2 showed a visible decline. Subsequently, in case of prediction modeling, the optimal 2HL-10N architecture provided high R values (0.99481 training, 0.9781 validation, 0.96914 testing, 0.98819 overall). The model maintained low RMSE and MSE values and predicted accurately. Afterward, Gradient-based optimization revealed the optimal condition for engine operation using HHO along with gasoline. The optimization yielded optimal conditions as 3.7 l/m HHO volume flow rate, 3700 rpm, and 100 % load. BP, and BTE improved by 11.4 %, and 7.1 % at the optimized input variables as compared to gasoline, respectively. BSFC, CO, CO_2, and HC emissions decreased by 11.5 %, 27.1 %, 7.6 %, and 36.6 % respectively. Enhanced hydrogen and oxygen quantity within induction charge managed better combustion and boosted heat along with discharge gas temperature. Consequently, an increment of 22.8 % in NOx emission content was recorded. A close alignment between test and optimized results validated the prediction and optimization using ANN and Gradient-based optimization. The very combination of ML techniques supports ethical production, sustainable operation, and informed decisions for enhanced engine efficiency and reduced emissions when fueled with gasoline and HHO mixture.

The current work has assessed the effect of renewable fuel on performance and emissions along with successful predication and optimization by utilizing ANN and Gradient-based optimization. However, the impact of hydrogen on the lubricating oil of engine by employing various speeds and operating hours may be considered for future work. Moreover, various optimization techniques and ANN models with diverse algorithms and training functions may also be applied for the optimization and predictions of thermal systems. Consequently, a good percentage of time and cost associated with lubricating oil testing will be saved. Combination of optimization and prediction with other techniques like transfer and reinforcement learning can establish a broader future of AI by developing systems that are more capable, responsive and adaptive. Also, investigating the economic feasibility and scalability of HHO production, storage, and distribution, alongside improved electrolysis and storage technologies, can offer insight into broader hydrogen fuel adoption.

CRediT authorship contribution statement

Muhammad Nasir Bashir: Writing – original draft, Methodology, Conceptualization. **Muhammad Usman:** Writing – original draft, Supervision, Investigation, Conceptualization. **Fahid Riaz:** Validation, Software, Funding acquisition. **Touqeer Ahmad:** Visualization, Software, Methodology. **Yasser Fouad:** Writing – review & editing, Resources, Funding acquisition, Data curation. **M. Shameer Basha:** Writing – review & editing, Visualization, Investigation. **Muhammad Mujtaba Abbas:** Validation, Formal analysis. **Joon Sang Lee:** Supervision, Resources, Formal analysis, Data curation.

Declaration of competing interest

The authors declare that they have no known competing financial interests or personal relationships that could have appeared to influence the work reported in this paper.

Acknowledgements

This work was supported by the National Research Foundation of Korea (NRF) grant funded by the Korea government. (MSIT) (2022R1A2C2092577). And partly supported by YFL 2024 yonsei university seoul, Korea. Also, the authors extend their appreciation to the Researchers Supporting Project number (RSPD2025R698), King Saud University, Riyadh, Saudi Arabia for funding this research work.

Data availability

Data will be made available on request.

References

[1] R.D. Reitz, H. Ogawa, R. Payri, T. Fansler, S. Kokjohn, Y. Moriyoshi, A. Agarwal, D. Arcoumanis, D. Assanis, C. Bae, IJER editorial: the future of the internal combustion engine, Int. J. Engine Res. 21 (1) (2020) 3–10.
[2] Z.U. Hassan, M. Usman, M. Asim, A.H. Kazim, M. Farooq, M. Umair, S.S. Asim, Use of diesel and emulsified diesel in CI engine: a comparative analysis of engine characteristics, Sci. Prog. 104 (2) (2021) 00368504211020930.
[3] S. Simsek, B. Ozdalyan, Improvements to the composition of fusel oil and analysis of the effects of fusel oil–gasoline blends on a spark-ignited (SI) engine's performance and emissions, Energies 11 (3) (2018) 625.
[4] L. Montanarella, R. Vargas, Global governance of soil resources as a necessary condition for sustainable development, Curr. Opin. Environ. Sustain. 4 (5) (2012) 559–564.
[5] E. Murphy, A. Banerjee, P.P. Walsh, Partnerships and the Sustainable Development Goals, Springer, 2022.
[6] K.G. Tsita, S.J. Kiartzis, N.K. Ntavos, P.A. Pilavachi, Next generation biofuels derived from thermal and chemical conversion of the Greek transport sector, Therm. Sci. Eng. Prog. 17 (2020) 100387.
[7] G. Kalghatgi, Developments in internal combustion engines and implications for combustion science and future transport fuels, Proc. Combust. Inst. 35 (1) (2015) 101–115.
[8] M. Aliramezani, C.R. Koch, M. Shahbakhti, Modeling, diagnostics, optimization, and control of internal combustion engines via modern machine learning techniques: a review and future directions, Prog. Energy Combust. Sci. 88 (2022) 100967.
[9] M. Acheampong, F.C. Ertem, B. Kappler, P. Neubauer, In pursuit of Sustainable Development Goal (SDG) number 7: will biofuels be reliable? Renew. Sustain. Energy Rev. 75 (2017) 927–937.
[10] Z.I. Rony, M. Mofijur, M. Hasan, M. Rasul, M. Jahirul, S.F. Ahmed, M. Kalam, I.A. Badruddin, T.Y. Khan, P.-L. Show, Alternative fuels to reduce greenhouse gas emissions from marine transport and promote UN sustainable development goals, Fuel 338 (2023) 127220.
[11] D. Akal, S. Öztuna, M.K. Büyükakın, A review of hydrogen usage in internal combustion engines (gasoline-Lpg-diesel) from combustion performance aspect, Int. J. Hydrogen Energy 45 (60) (2020) 35257–35268.
[12] A. Ahmed, A.Q. Al-Amin, A.F. Ambrose, R. Saidur, Hydrogen fuel and transport system: A sustainable and environmental future, International journal of hydrogen energy 41 (3) (2016) 1369–1380.
[13] N. Armaroli, V. Balzani, The hydrogen issue, ChemSusChem 4 (1) (2011) 21–36.
[14] X. Zhen, X. Li, Y. Wang, D. Liu, Z. Tian, Comparative study on combustion and emission characteristics of methanol/hydrogen, ethanol/hydrogen and methane/hydrogen blends in high compression ratio SI engine, Fuel 267 (2020) 117193.
[15] C.-z. Zhu, O.D. Samuel, N. Elboughdiri, M. Abbas, C.A. Saleel, N. Ganesan, C.C. Enweremadu, H. Fayaz, Artificial neural networks vs. gene expression programming for predicting emission & engine efficiency of SI operated on blends of gasoline-methanol-hydrogen fuel, Case Stud. Therm. Eng. 49 (2023) 103109.
[16] P.K. Sharma, D. Sharma, S.L. Soni, A. Jhalani, D. Singh, S. Sharma, Energy, exergy, and emission analysis of a hydroxyl fueled compression ignition engine under dual fuel mode, Fuel 265 (2020) 116923.
[17] S. Thangaraj, N. Govindan, Investigating the pros and cons of browns gas and varying EGR on combustion, performance, and emission characteristics of diesel engine, Environ. Sci. Pollut. Control Ser. 25 (1) (2018) 422–435.
[18] M. Gad, S.A. Razek, Impact of HHO produced from dry and wet cell electrolyzers on diesel engine performance, emissions and combustion characteristics, Int. J. Hydrogen Energy 46 (43) (2021) 22277–22291.
[19] J. Babu, K.S. Kumar, R.R. Kumar, Ü. Ağbulut, A. Razak, D. Thakur, V. Sundara, M. Asif, Production of HHO gas in the water-electrolysis unit and the influences of its introduction to CI engine along with diesel-biodiesel blends at varying injection pressures, Int. J. Hydrogen Energy 52 (2024) 865–885.
[20] T. Wajda, K. Gabriel, Thermolysis reactor scale-up for pilot scale CuCl hybrid hydrogen production, Int. J. Hydrogen Energy 44 (20) (2019) 9779–9790.
[21] K.C. Christoforidis, P. Fornasiero, Photocatalytic hydrogen production: a rift into the future energy supply, ChemCatChem 9 (9) (2017) 1523–1544.
[22] S. Wang, D. Zhang, X. Ma, J. Liu, Y. Chen, Y. Zhao, Y. Han, Modifying ionic membranes with carbon dots enables direct production of high-purity hydrogen through water electrolysis, ACS Appl. Mater. Interfaces 13 (33) (2021) 39304–39310.
[23] K. Zeng, D. Zhang, Recent progress in alkaline water electrolysis for hydrogen production and applications, Prog. Energy Combust. Sci. 36 (3) (2010) 307–326.

[24] S. Wang, C. Ji, B. Zhang, X. Liu, Performance of a hydroxygen-blended gasoline engine at different hydrogen volume fractions in the hydroxygen, Int. J. Hydrogen Energy 37 (17) (2012) 13209–13218.
[25] M.M. El-Kassaby, Y.A. Eldrainy, M.E. Khidr, K.I. Khidr, Effect of hydroxy (HHO) gas addition on gasoline engine performance and emissions, Alex. Eng. J. 55 (1) (2016) 243–251.
[26] A. Falahat, M. Hamdan, J. Yamin, Engine performance powered by a mixture of hydrogen and oxygen fuel obtained from water electrolysis, Int. J. Automot. Technol. 15 (2014) 97–101.
[27] V.M. Krishna, A.H. Reddy, M.S. Kumar, A. Raghu, Effect of hydroxy gas addition on performance and exhaust emissions in variable compression spark ignition engine, Mater. Today: Proc. 24 (2020) 930–936.
[28] T. Shinagawa, K. Takanabe, Towards versatile and sustainable hydrogen production through electrocatalytic water splitting: electrolyte engineering, ChemSusChem 10 (7) (2017) 1318–1336.
[29] M. Schalenbach, G. Tjarks, M. Carmo, W. Lueke, M. Mueller, D. Stolten, Acidic or alkaline? Towards a new perspective on the efficiency of water electrolysis, J. Electrochem. Soc. 163 (11) (2016) F3197.
[30] T. Nabil, M.M.K. Dawood, Enabling efficient use of oxy-hydrogen gas (HHO) in selected engineering applications; transportation and sustainable power generation, J. Clean. Prod. 237 (2019) 117798.
[31] S. Wang, C. Ji, J. Zhang, B. Zhang, Improving the performance of a gasoline engine with the addition of hydrogen–oxygen mixtures, Int. J. Hydrogen Energy 36 (17) (2011) 11164–11173.
[32] A.A. Al-Rousan, Reduction of fuel consumption in gasoline engines by introducing HHO gas into intake manifold, Int. J. Hydrogen Energy 35 (23) (2010) 12930–12935.
[33] N. Patil, C. Chavan, A. More, P. Baskar, Generation of oxy-hydrogen gas and its effect on performance of spark ignition engine, IOP Conf. Ser. Mater. Sci. Eng. 263 (6) (2017) 062036.
[34] A. Sa'ed, A.A. Al-Rousan, Effect of HHO gas on combustion emissions in gasoline engines, Fuel 90 (10) (2011) 3066–3070.
[35] V.M. Krishna, R.A. Haritha, K.M. Sandeep, A. Raghu, Effect of hydroxy gas addition on performance and exhaust emissions in variable compression spark ignition engine, Mater. Today: Proc. 24 (2020) 930–936.
[36] Y. Karagöz, L. Yüksek, T. Sandalcı, A.S. Dalkılıç, An experimental investigation on the performance characteristics of a hydroxygen enriched gasoline engine with water injection, Int. J. Hydrogen Energy 40 (1) (2015) 692–702.
[37] A.A. Al-Rousan, S.A. Musmar, Effect of anodes-cathodes inter-distances of HHO fuel cell on gasoline engine performance operating by a blend of HHO, Int. J. Hydrogen Energy 43 (41) (2018) 19213–19221.
[38] V.M. Krishna, Emissions control and performance evaluation of spark ignition engine with oxy-hydrogen blending, International Journal of Heat and Technology 36 (1) (2018) 118–124.
[39] S. Wang, J. Changwei, Z. Jian, Z. Bo, Comparison of the performance of a spark-ignited gasoline engine blended with hydrogen and hydrogen–oxygen mixtures, Energy 36 (10) (2011) 5832–5837.
[40] A.A. Al-Rousan, S. Alkheder, S.A. Musmar, Urban traffic pollution reduction for sedan cars using petrol engines by hydro-oxide gas inclusion, J. Air Waste Manag. Assoc. 65 (12) (2015) 1456–1460.
[41] Z. Zhao, H. Yan, Y. Xiumin, L. Ming, Z. Zhihong, G. Zezhou, W. Tianqi, L. Decheng, Comparative study on combustion and emission of SI engine blended with HHO by different injection modes of gasoline, Int. J. Hydrogen Energy 47 (80) (2022) 34273–34290.
[42] Y. Karagöz, N. Yuca, T. Sandalcı, A.S. Dalkılıç, Effect of hydrogen and oxygen addition as a mixture on emissions and performance characteristics of a gasoline engine, Int. J. Hydrogen Energy 40 (28) (2015) 8750–8760.
[43] T. Le Anh, K. Nguyen Duc, H. Tran Thi Thu, T. Cao Van, Improving performance and reducing pollution emissions of a carburetor gasoline engine by adding HHO gas into the intake manifold, SAE Technical Paper 2013-01-0104 (2013).
[44] M.M. El-Kassaby, A.E. Yehia, E.K. Mohamed, I.K. Kareem, Effect of hydroxy (HHO) gas addition on gasoline engine performance and emissions, Alex. Eng. J. 55 (1) (2016) 243–251.
[45] Y. Gutarevych, S. Yevheniy, M. Jonas, K. Stanislav, S. Edgar, R. Alfredas, Intensification of the combustion process in a gasoline engine by adding a hydrogen-containing gas, Int. J. Hydrogen Energy 43 (33) (2018) 16334–16343.
[46] M. Aminy, M. Ghomashi, K. Abbaspour-sani, L.T. Savadkohi, An investigate on power, torque and exhaust gas emission variation: effect of hydroxy gas addition to inlet air of a SI engine, International Journal of Engineering, Transactions B: Applications 27 (2014) 1751–1756.
[47] J. Fu, R. Yang, X. Li, X. Sun, Y. Li, Z. Liu, Y. Zhang, B. Sunden, Application of artificial neural network to forecast engine performance and emissions of a spark ignition engine, Appl. Therm. Eng. 201 (2022) 117749.
[48] Z. Liu, J. Liu, Machine learning assisted analysis of an ammonia engine performance, J. Energy Resour. Technol. 144 (11) (2022) 112307.
[49] J. Liu, Q. Huang, C. Ulishney, C.E. Dumitrescu, Comparison of random forest and neural network in modeling the performance and emissions of a natural gas spark ignition engine, J. Energy Resour. Technol. 144 (3) (2022) 032310.
[50] Q. Huang, J. Liu, C. Ulishney, C.E. Dumitrescu, On the use of artificial neural networks to model the performance and emissions of a heavy-duty natural gas spark ignition engine, Int. J. Engine Res. 23 (11) (2022) 1879–1898.
[51] P. Sun, J. Zhang, W. Dong, D. Li, X. Yu, Prediction of oxygen-enriched combustion and emission performance on a spark ignition engine using artificial neural networks, Appl. Energy 348 (2023) 121466.
[52] O.D. Samuel, M.O. Okwu, L.K. Tartibu, S.O. Giwa, M. Sharifpur, Z.O. Jagun, Modelling of Nicotiana tabacum L. oil biodiesel production: comparison of ANN and ANFIS, Front. Energy Res. 8 (2021) 612165.
[53] M. Usman, N. Hayat, M.M.A. Bhutta, SI engine fueled with gasoline, CNG and CNG-HHO blend: comparative evaluation of performance, emission and lubrication oil deterioration, J. Therm. Sci. 30 (4) (2021) 1199–1211.
[54] M. Brayek, M.A. Jemni, G. Kantchev, M.S. Abid, Effect of hydrogen–oxygen mixture addition on exhaust emissions and performance of a spark ignition engine, Arabian J. Sci. Eng. 41 (2016) 4635–4642.
[55] M.A.R.S. Al-Baghdadi, Performance study of a four-stroke spark ignition engine working with both of hydrogen and ethyl alcohol as supplementary fuel, Int. J. Hydrogen Energy 25 (10) (2000) 1005–1009.
[56] B. Subramanian, S. Ismail, Production and use of HHO gas in IC engines, Int. J. Hydrogen Energy 43 (14) (2018) 7140–7154.
[57] G.J. Delagrammatikas, D.N. Assanis, Development of a neural network model of an advanced, turbocharged diesel engine for use in vehicle-level optimization studies, Proc. Inst. Mech. Eng. - Part D J. Automob. Eng. 218 (5) (2004) 521–533.
[58] S.A. Kalogirou, Artificial intelligence for the modeling and control of combustion processes: a review, Prog. Energy Combust. Sci. 29 (6) (2003) 515–566.
[59] I. Papadimitriou, M. Warner, J. Silvestri, J. Lennblad, S. Tabar, Neural network based fast-running engine models for control-oriented applications, SAE Technical Paper: 2005-01-0072 (2005).
[60] M. Aydın, S. Uslu, M.B. Çelik, Performance and emission prediction of a compression ignition engine fueled with biodiesel-diesel blends: a combined application of ANN and RSM based optimization, Fuel 269 (2020) 117472.
[61] M. Ćalasan, S.H.E. Abdel Aleem, A.F. Zobaa, On the root mean square error (RMSE) calculation for parameter estimation of photovoltaic models: a novel exact analytical solution based on Lambert W function, Energy Convers. Manag. 210 (2020) 112716.
[62] Z. Zhao, L. Alzubaidi, J. Zhang, Y. Duan, Y. Gu, A comparison review of transfer learning and self-supervised learning: definitions, applications, advantages and limitations, Expert Syst. Appl. 242 (2024) 122807.
[63] R. Kenanoğlu, M.K. Baltacıoğlu, M.H. Demir, M.E. Özdemir, Performance & emission analysis of HHO enriched dual-fuelled diesel engine with artificial neural network prediction approaches, Int. J. Hydrogen Energy 45 (49) (2020) 26357–26369.
[64] D.Y. Dhande, C.S. Choudhari, D.P. Gaikwad, K.B. Dahe, Development of artificial neural network to predict the performance of spark ignition engine fuelled with waste pomegranate ethanol blends, Information Processing in Agriculture 10 (4) (2023) 459–474.

[65] M. Deb, P. Majumder, A. Majumder, S. Roy, R. Banerjee, Application of artificial intelligence (AI) in characterization of the performance–emission profile of a single cylinder CI engine operating with hydrogen in dual fuel mode: an ANN approach with fuzzy-logic based topology optimization, Int. J. Hydrogen Energy 41 (32) (2016) 14330–14350.
[66] N. Ganesan, S. Ishan, O.D. Samuel, C.C. Enweremadu, I. Veza, D. Chandran, Optimization and sustainability of gasohol/hydrogen blends for operative spark ignition engine utilization and green environment, Case Stud. Therm. Eng. 39 (2022) 102381.
[67] O.D. Samuel, M.A. Waheed, A. Taheri-Garavand, T.N. Verma, O.U. Dairo, B.O. Bolaji, A. Afzal, Prandtl number of optimum biodiesel from food industrial waste oil and diesel fuel blend for diesel engine, Fuel 285 (2021) 119049.
[68] A. Taheri-Garavand, A. Heidari-Maleni, T. Mesri-Gundoshmian, O.D. Samuel, Application of artificial neural networks for the prediction of performance and exhaust emissions in IC engine using biodiesel-diesel blends containing quantum dot based on carbon doped, Energy Convers. Manag. X 16 (2022) 100304.